AJNR

Contrast-enhanced three-dimensional fast imaging with steady-state precession (FISP) MR angiography of supraaortic vessels: preliminary results.

X Leclerc, P Martinat, O Godefroy, C Lucas, F Giboreau, G S Ares, D Leys and J P Pruvo

AJNR Am J Neuroradiol 1998, 19 (8) 1405-1413
http://www.ajnr.org/content/19/8/1405

AJNR Am J Neuroradiol 19:1405–1413, September 1998

Contrast-Enhanced Three-Dimensional Fast Imaging with Steady-State Precession (FISP) MR Angiography of Supraaortic Vessels: Preliminary Results

Xavier Leclerc, Pascal Martinat, Olivier Godefroy, Christian Lucas, Frederic Giboreau, Gustavo Soto Ares, Didier Leys, and Jean-Pierre Pruvo

BACKGROUND AND PURPOSE: **The purpose of this study was to assess the effectiveness of contrast-enhanced fast three-dimensional (3D) MR angiography in depicting both the carotid and vertebral arteries in their cervical portions and to compare MR angiography with conventional angiography for the evaluation of arteriosclerotic disease.**

METHODS: **Twenty-seven patients with ischemic cerebral events in the anterior (n = 18) and posterior (n = 9) circulation underwent contrast-enhanced 3D MR angiography in the coronal plane. MR angiograms were examined in a blinded fashion by two observers independently. Stenosis was classified according to the appearance of the residual lumen (no stenosis, mild stenosis, moderate stenosis, severe stenosis, occlusion). Conventional angiography was used as the standard of reference.**

RESULTS: **Proximal great vessels and carotid siphons were not assessable on MR angiograms in 35% of cases owing to limited coverage. All cervical and petrous segments of the internal carotid arteries (ICAs) and 93% of the extracranial vertebral arteries were assessable. Flow-related artifacts were observed in seven cases of severe stenosis, including three with signal void at the site of narrowing and four with signal loss in the distal ICA. Interobserver agreement was good and significant. Overall agreement between 3D MR angiography and conventional angiography was good for the anterior and posterior circulations despite a tendency toward overestimation of stenoses on MR angiograms. Clinically relevant stenoses and occlusions were correctly identified on 3D MR angiograms, providing good sensitivity and specificity.**

CONCLUSION: **Contrast-enhanced 3D MR angiography is a promising tool for assessing arteriosclerotic lesions of supraaortic vessels. Further studies with larger groups are required to determine its value for patient care.**

Conventional angiography is considered the standard of reference for evaluating arteriosclerotic lesions of the supraaortic extracranial vessels and especially for detecting stenosis of the internal carotid artery (ICA) (1, 2). However, this technique carries a risk of complications related to thromboembolic events, allergic reactions, and nephrotoxicity (3). Thus, noninvasive techniques, such as duplex sonography, helical CT, and MR angiography, need to be considered as an alternative to conventional angiography whenever possible.

It has been shown that three-dimensional (3D) time-of-flight (TOF) MR angiography is effective in depicting high-grade carotid stenoses (4–7) with very good sensitivity and specificity, especially when the phase-contrast technique is used (7); however, coverage remains limited and evaluation of both the anterior and posterior circulations is not possible, although the development of new MR angiographic techniques may circumvent this persisting drawback. The objective of replacing most angiographic studies with MR angiography awaits the development of new

Received January 12, 1998; accepted after revision May 1.

From the Departments of Radiology (X.L., P.M., G.S.A., J-P.P.) and Neurology (O.G., C.L., D.L.), University Hospital of Lille (France); and the Research Laboratory, Siemens Medical Systems, Erlangen, Germany (F.G.).

Address reprint requests to X. Leclerc, MD, Service de Neuroradiologie, Hôpital Roger Salengro, Boulevard du Professeur Leclercq, 59037, Lille, France.

sequences that would allow the evaluation of all extracranial vessels in patients with ischemia.

Some studies have reported the use of contrast-enhanced MR angiography as a means to improve vascular conspicuity (8–11). Promising results have been reported by one group of investigators (12–15) who used a contrast-enhanced fast 3D gradient-echo technique with a short scanning time to image vascular structures. The principle is based on a maximum saturation effect achieved with the use of a short repetition time (TR) of 5 to 10 milliseconds, so that the T1 relaxation of spins, including blood and fat, remains higher than the TR. If contrast material is infused and correctly timed, the major shortening of blood T1 results in high signal intensity of the vascular structures. Image contrast is less influenced by inflow effects, so the 3D slab may be oriented in any direction and a larger volume may be examined. However, to selectively enhance the arterial phase, accurate timing of contrast infusion is required. Some methods have recently been described to increase contrast resolution; for example, a test bolus can be administered before 3D MR angiography to calculate the transit time (16), an automatic power injector may be useful for achieving reproducible contrast infusion (17), and a fluoroscopically triggered MR angiographic sequence may improve the ability to isolate the arterial phase (18). Contrast MR angiography has proved valuable in the analysis of the aorta and its major branches (12, 19), and a recent study suggested that it is capable of selectively enhancing the arterial phase of carotid arteries (13). However, for head and neck evaluation, no clinical findings have yet been reported.

The purpose of this preliminary study was to assess the value of contrast-enhanced 3D fast imaging with steady-state precession (FISP) MR angiography for examining the extracranial supraaortic vessels in patients with arteriosclerotic disease.

Methods

Patients

From February to July 1997, 27 patients with an ischemic cerebral event in the anterior or posterior circulation underwent MR imaging and conventional angiography. The study group consisted of 10 women and 17 men, 41 to 82 years old (median age, 62 years), with history of hemispheric ischemia in 18 and cerebellar and/or brain stem ischemia in nine. Ten patients had clinical evidence of a transient ischemic attack. All patients underwent Doppler sonography and were referred from the neurology department for MR imaging and conventional angiography. Both examinations were performed within a 1-month period following onset of symptoms. Angiograms were obtained with a digital subtraction technique through a femoral approach. Arch aortograms with two oblique cervical projections were followed by selective catheterization of the common carotid artery or the subclavian artery or both to evaluate the exact degree of ICA or vertebral artery stenosis. Selective catheterization of the vertebral artery was not performed and, therefore, the intracranial portion of the vertebral artery was not visualized. Carotid angiograms included cervical and head views. The contrast dose for the entire study did not exceed 150 mL (Omnipaque 300, Nycomed).

Imaging Technique

MR angiography was performed with a 1.5-T superconductive unit with the use of a head and neck coil. Prior to imaging, a transverse two-dimensional (2D) TOF sequence of the neck was obtained to include both carotid and vertebral arteries in the 3D slab. Twenty sections were acquired from the upper portion of the aortic arch to the skull base with the following parameters: 27/17/1 (TR/TE/excitations), 3-mm section thickness, 50° flip angle, 25-cm field of view, and 128 × 256 matrix. We used an axial saturation band over the intracranial dural venous sinuses to eliminate signal from the veins. Image acquisition time was 1 minute 30 seconds.

Contrast-enhanced 3D MR angiography was performed in the coronal plane using a FISP sequence. The small diameter of the cervical arteries required us to adapt this sequence to the neck by making a compromise between spatial resolution, acquisition time, and imaging volume. Parameters were standardized for a systematic evaluation. Section thickness was 1.5 mm with 40 partitions obtained in the coronal plane, allowing an anteroposterior coverage of 60 mm. The TR/TE was reduced to 5/2. Other parameters included a 35° flip angle, a 100% zero-filling interpolation, a fat-saturation sequence, and a field of view of 35 cm with a 200 × 256 matrix, leading to a pixel size of 1.31 × 1.27 mm. The entire volume was acquired in 44 seconds. A precontrast sequence was performed in each case to ensure that the volume was correctly positioned.

Contrast Infusion

The contrast material (gadodiamide, Omniscan, Nycomed, Princeton, NJ) was infused by hand injection through a 22-gauge venous angiocatheter in the antecubital fossa. After prefilling the connecting tube with 5 mL of contrast material, 20 mL (10 mmol) was injected at a rate of approximately 1 mL/s by a radiologist standing in the imaging room. Contrast infusion was immediately followed by injection of 20 mL of normal saline to flush the veins. Injection of contrast material was timed so that the arterial phase occurred midway during the course of the acquisition. No test bolus was used to time the acquisition. In most cases, injection was started at the beginning of the sequence. This delay was lengthened (5 seconds) in patients older than 60 years of age. When no hypersignal was detected in the ICA or when the signal in the jugular vein was higher than that in the ICA, the sequence was repeated 5 to 10 minutes later using an additional 20-mL dose of contrast material and a modified scan delay between the start of the injection and the start of the sequence (5- to 10-second increments when no arterial enhancement was obtained and 5- to 10-second decrements in cases of major venous enhancement).

Image Reconstruction

Data were transferred to an independent workstation, and subvolumes were generated to isolate both carotid and vertebral arteries. When stenosis was detected, selective subvolume and magnification were created. MR angiograms were displayed by the use of a maximum-intensity-projection (MIP) algorithm. Lateral rotations were obtained every 10°, from −90° to +90°, with 0° corresponding to the frontal plane. After the images were evaluated on the console, nine views were exposed on a laser film. Reconstructions were performed without knowledge of the angiographic data.

Image Analysis

Conventional angiography was interpreted in a consensual manner by two senior neuroradiologists who were blinded to the results of MR angiography. The degree of stenosis was measured by comparing the diameter of the residual lumen at its narrowest point with the diameter of the distal portion of the artery (1). Measurement was not performed in cases of

TABLE 1: Technical considerations of fast 3D contrast-enhanced MR angiography for the evaluation of extracranial vessels

Arterial Portions	No. of Arteries	No.	MR Angiography				
			Nonassessable		No.	Assessable	
			Inadequate Coverage	Low Contrast		Mild Contrast	Good Contrast
BCA	27	12	9	3	15	4	11
SCA	54	14	12	2	40	7	33
CCA	54	21	19	2	33	9	24
ICA	54	0	...	...	54	4	50
CS	54	19	18	1	35	6	29
VA	54	4	1	3	50	16	34
Total	297	70	59	11	227	46	181

Note.—BCA indicates brachiocephalic artery; SCA, subclavian artery; CCA, common carotid artery; ICA, cervical and petrous segments of the internal carotid artery; CS, carotid siphon; VA, vertebral artery.

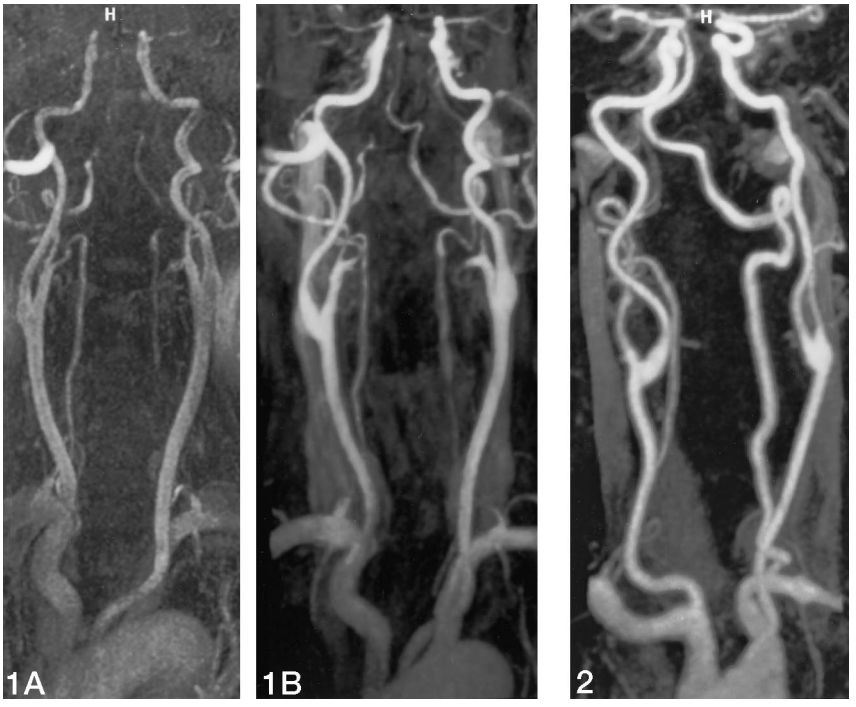

FIG 1. *A*, MR angiogram of supraaortic vessels with bolus injection of contrast material starting at the beginning of the sequence shows poor vascular contrast owing to a lack of signal intensity in both carotid and vertebral arteries.

B, An additional MR angiogram obtained 5 minutes later with contrast infusion starting 10 seconds before the sequence shows adequate arterial enhancement.

FIG 2. Normal contrast-enhanced MR angiogram with bolus injection of contrast material starting at the beginning of the sequence (44-second scan time) clearly depicts supraaortic vessels from the arch to the circle of Willis.

hairline residual lumen or when the artery appeared normal or occluded. Arteries of the anterior circulation were then assigned to one of five categories: no stenosis, mild stenosis (<30%), moderate stenosis (30% to 70%), severe stenosis (>70%), and occlusion. Stenoses higher than 70% were considered clinically relevant (1, 2). The absence of a trial for clinically relevant vertebral stenosis led us to modify the gradations according to hemodynamic criteria (20), as follows: no stenosis, mild stenosis (<50%), moderate stenosis (50% to 70%), severe stenosis (>70%), and occlusion. Vertebral artery stenosis higher than 50% was considered clinically significant, as hemodynamic changes occur with a 50% reduction in diameter (20). The quality of MR angiograms was evaluated in a consensual manner using the following four criteria: image coverage, arterial signal, venous signal, and presence of artifacts. Analysis was performed in six arterial locations: the brachiocephalic artery, the subclavian artery, the common carotid artery, the cervical portion of the ICA, the extracranial vertebral artery, and the carotid siphon. The intracranial portion of the vertebral artery was not evaluated in our study owing to the absence of a direct comparison with findings on conventional angiograms. When a part of the artery was not included in the imaging volume, the artery was judged nonassessable. Arterial-phase enhancement was graded as 0 (low), 1 (mild), or 2 (good), and the image was judged nonassessable in cases of low contrast. Signal intensity in the jugular vein was graded as 0 (no enhancement), 1 (mild), or 2 (moderate). When venous signal was graded as high, an additional contrast-enhanced MR angiographic sequence was performed. Artifactual evaluation included the presence of motion artifacts, flow-related artifacts, skull base induced–artifacts, and longitudinal linear artifacts.

When the artery was judged assessable, stenoses were categorized in a blinded fashion by two trained radiologists who separately reviewed the MR angiograms in a fully randomized order. No direct measurement of the stenosis was made on MR angiograms owing to the large voxel size, which did not allow an accurate delineation of the arteries. We compared the narrowest diameter of the residual lumen with the diameter of the normal artery well beyond the stenosis. Each artery was then assigned to one of the categories described for conventional angiography; that is, no stenosis, mild stenosis, moderate

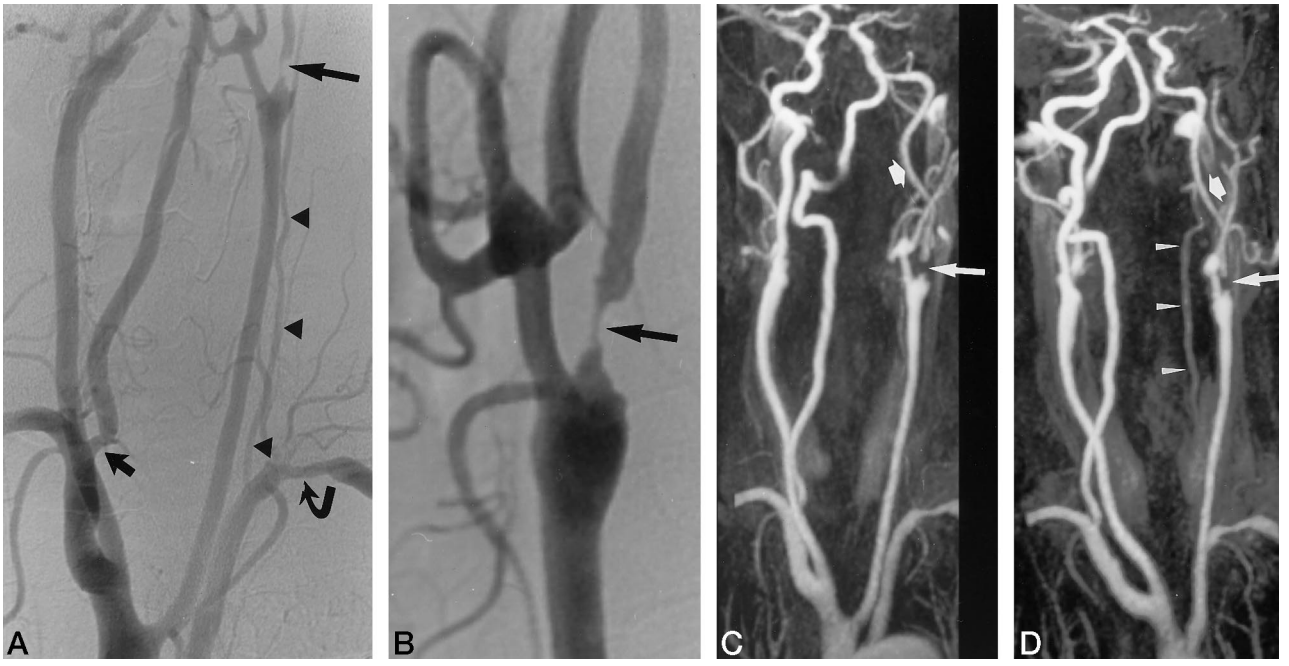

FIG 3. *A* and *B*, Arch aortogram (*A*) and selective angiogram (*B*) of the left carotid artery reveal a dominant right vertebral artery with mild stenosis at its origin (*short arrow*), a small left vertebral artery (*arrowheads*), moderate stenosis of the left subclavian artery (*curved arrow*), and nearly occlusive stenosis of the left ICA (*long arrow*).

C and *D*, Contrast-enhanced MR angiograms show a signal void at the origin of the left ICA (*long arrow*) and signal loss in its distal portion (short arrow). The transverse segment of the left vertebral artery can be evaluated (*arrowheads*), whereas its proximal segment is not visible.

FIG 4. *A* and *B,* Arch aortogram *(A)* and selective angiogram *(B)* of the left ICA reveal severe stenosis at the origin of the right vertebral artery *(arrow)* and 60% stenosis of the left ICA with a long and irregular narrowing *(arrowheads)*. *C,* MR angiogram shows an overestimation of the left ICA stenosis, which appears to be severe *(arrow)*, and a signal void at the origin of the right vertebral artery *(arrowhead)*.

stenosis, severe stenosis, or occlusion. The stenosis was judged as mild when irregularities of the arterial wall were observed, moderate when the residual lumen appeared slightly narrowed, severe when a thin linear hypersignal or signal void was observed at the site of the stenosis, and occluded if no signal was seen in the expected course of the artery.

Statistical Analysis

The first step of the analysis consisted of an evaluation of the level of interobserver agreement for assessable contrast-enhanced fast 3D MR angiograms by means of the κ statistic (21). In the second step we assessed the agreement between MR angiography and conventional angiography in terms of stenosis categorization (no stenosis, mild stenosis, moderate stenosis, severe stenosis, or occlusion) using κ statistics. κ statistics were calculated separately for the anterior and posterior circulations. κ values between .4 and .8 suggested a moderate to substantial agreement, and values higher than .8 indicated excellent agreement. *P* values lower than .05 were regarded as significant. Finally, the usefulness of MR angiography for the detection of occlusion, clinically relevant stenosis of the ICA (sever stenosis), and ostial vertebral artery (moderate or severe) stenosis was assessed by use of Fisher's exact test (22).

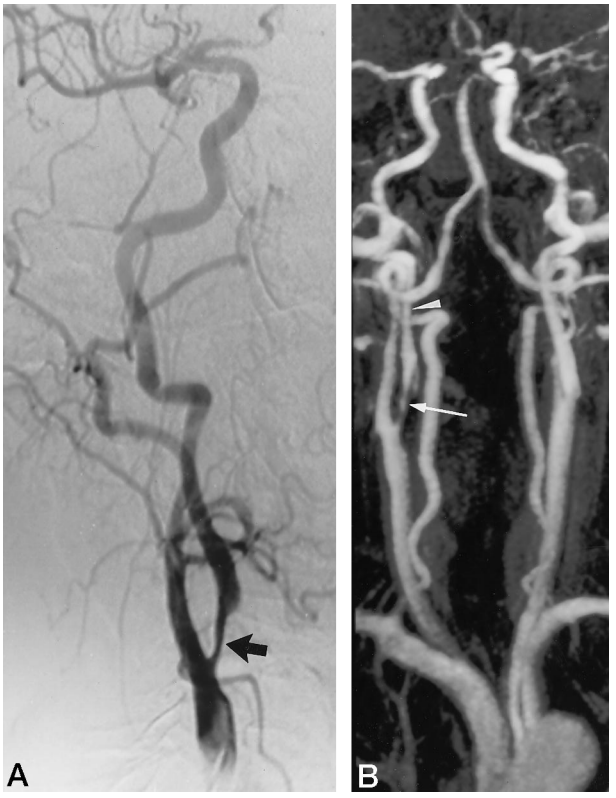

FIG 5. *A*, Selective conventional angiogram of the right carotid artery shows an 80% diameter long stenosis at the origin of the ICA (*arrow*) with a normal distal ICA.

B, MR angiogram shows a similar appearance of the stenosis (*arrow*) and a signal loss of the ICA beyond the narrowing (*arrowhead*).

FIG 6. *A*, Conventional arch aortogram shows a 20% diameter stenosis at the origin of the right ICA (*arrow*).

B, Contrast-enhanced MR angiogram shows a right ICA stenosis (*arrow*) in accordance with conventional angiography.

Results

Technical Considerations of Fast 3D Contrast-Enhanced MR Angiography (Table 1)

A second contrast-enhanced MR angiographic sequence was performed in six patients (22%) owing to a lack of signal from the ICA in two patients (7%) (Fig 1) and to a high signal from the jugular vein in four patients (15%). The additional sequence, performed with modified timing, led to adequate arterial-phase enhancement in all cases. No contrast reaction or other adverse event was observed. Motion artifacts slightly degraded three examinations but did not prevent analysis.

Among the 135 proximal great vessels examined (brachiocephalic, subclavian, and common carotid arteries) in 27 patients, MR angiography failed to show the ostium in 47 cases (35%), including 21 common carotid arteries. Nineteen (35%) of the carotid siphons were not assessable. This was related to the limited imaging volume in 59 cases (84%) and to the low contrast in 11 other cases (16%). The cervical and petrous segments of the ICA were assessable in all cases. The proximal portion of the vertebral artery was not assessable in four patients (7%) owing to low contrast enhancement at the site of the ostium in three cases.

In the group of assessable arteries (n = 227), the arterial-phase enhancement was judged to be good by both observers in 181 cases (80%), including 50 ICAs (93%) (Fig 2). Complete isolation of the arterial phase (no enhancement of venous structures) was achieved in five patients (19%), whereas the jugular vein was mildly enhanced in 10 (37%) and moderately enhanced in 12 (44%); however, in no case did this prevent analysis of the carotid artery.

No in-plane saturation, skull base–induced artifacts, or longitudinal artifacts were found. However, flow-related artifacts were observed in seven instances of severe stenosis, including three cases of signal void at the site of narrowing (two in the ICA and one in the vertebral artery) (Figs 3 and 4) and four cases of signal loss in the distal ICA beyond the stenosis (Figs 3 and 5).

Interobserver Agreement for MR Angiographic Findings

Of the remaining group of 227 assessable arteries, interobserver agreement for classification of the anterior circulation on MR angiograms was judged as good and significant ($\kappa = .91$, $P < .0001$). However, discrepancies between the normal group and the group with mild stenosis were observed in five cases, including two in the common carotid artery and three in the ICA. In the posterior circulation, the overall interobserver agreement was significant as well ($\kappa = .79$, $P < .0001$). However, discrepancies between the normal group and the group with mild stenosis were observed in six cases (two in the subclavian artery and four in the vertebral artery) and between the moderate and severe groups, in one case of vertebral artery

FIG 7. *A*, Selective conventional angiogram reveals a 35% diameter stenosis of the ICA (*arrow*).
B, MR angiogram allowed correct grading of the stenosis (*arrow*) despite a mild overestimation.

stenosis. Images that provoked disagreement between the observers were reevaluated in order to reach a consensus.

Overall Agreement between MR Angiography and Conventional Angiography

The overall agreement between MR angiography and conventional angiography was good and significant in both the anterior circulation ($\kappa = .90$, $P < .0001$) (Figs 6 and 7) and the posterior circulation ($\kappa = .85$, $P < .0001$) (Fig 8). This good agreement between the techniques indicates that MR angiography is useful in the classification of carotid and vertebral stenoses. However, some discrepancies were observed, which are detailed in the following sections.

Proximal Great Vessels and Carotid Siphon (Table 2)

All brachiocephalic arteries and all carotid siphons were correctly classified from MR angiograms, including one mild stenosis of the brachiocephalic artery and five occlusions of the carotid siphon. One case of moderate stenosis of the subclavian artery and one case of severe stenosis in the distal portion of the common carotid artery were correctly detected. However, one mild stenosis of the subclavian artery and one normal common carotid artery were misclassified owing to overestimation of stenosis on MR angiograms.

Extracranial ICA (Table 3)

The six cases of ICA occlusion and the 10 cases of severe stenosis at the origin of the ICA were correctly identified on MR angiograms. However, five ICA stenoses were misclassified, including overestimations in two cases of mild stenosis and in one case of moderate stenosis. In one case of severe ICA stenosis, ulceration was well seen on both conventional and MR angiograms.

Extracranial Vertebral Artery (Table 4)

The only case of vertebral artery occlusion assessable on MR angiograms was diagnosed correctly. The three cases of vertebral artery stenosis with a narrowing in diameter of more than 50% were identified correctly on MR angiograms. However, four vertebral arteries were misclassified owing to an overestimation of stenosis on MR angiograms, including three normal vertebral arteries misclassified as mild or moderate stenosis.

Sensitivity and Specificity of MR Angiography for the Evaluation of Clinically Relevant Stenosis and ICA Occlusion (Table 5)

The sensitivity and specificity of MR angiography in detecting clinically relevant stenosis of the ICA (stenosis >70%), extracranial ICA occlusion, or hemodynamically significant stenosis of the vertebral artery (stenosis >50%) were found to be very good (Fisher's exact test: $P < .00001$), although one case of moderate stenosis of the ICA and one case of moderate stenosis of the vertebral artery were classified as severe on MR angiograms.

Discussion

The contrast-enhanced 3D fast MR angiographic sequences used in this study allowed the assessment of supraaortic vessels from the proximal portion of the great vessels to the carotid siphons in 65% of cases. All ICAs and 93% of vertebral arteries were assessable, with good interobserver agreement, indicating that image quality provided reliable analysis despite the frequent overestimation of mild stenosis. Finally, sensitivity and specificity for detecting relevant stenosis and occlusion of the ICA were very good.

In a previous study evaluating arterial-phase enhancement of cervical arteries with the use of contrast-enhanced MR angiography, Levy et al (13) underlined the importance of thin sections and a large 3D slab to achieve adequate spatial resolution of the carotid arteries. In the present study, we attempted to optimize the parameters of a 3D FISP sequence for assessing the cervical arteries. FISP is one of the fast-field-echo techniques based on the principle of coherent steady-state magnetization after radio-frequency excitation (23). A reverse phase-encoding gradient restores transverse magnetization, which allows the rephasing of stationary spins. We modified the

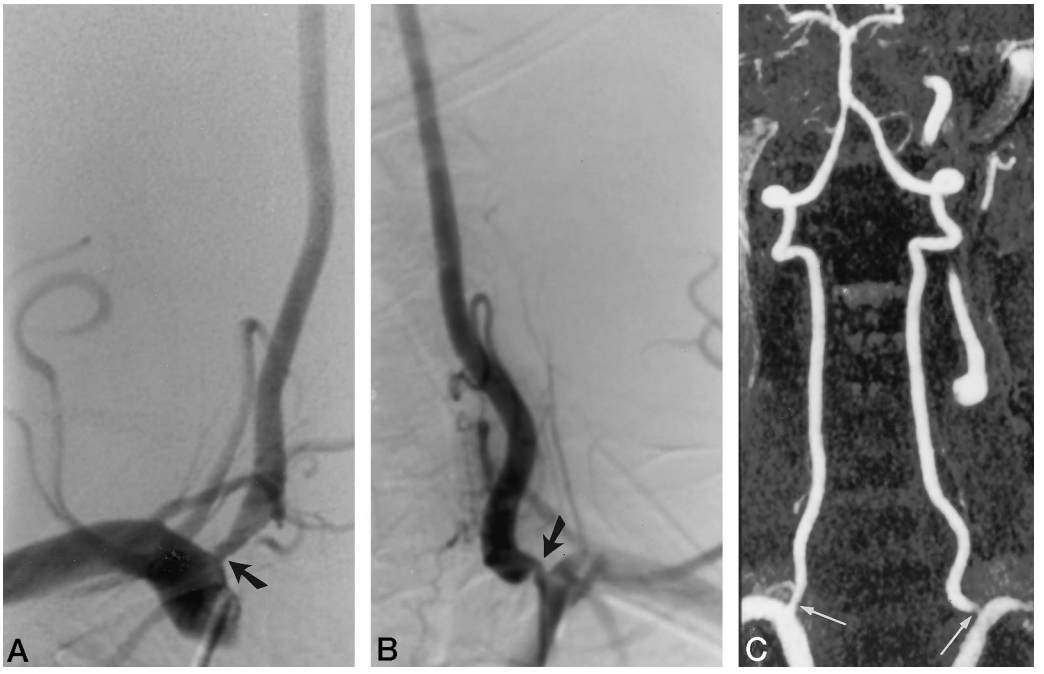

FIG 8. *A* and *B,* Selective conventional angiograms of the right *(A)* and left *(B)* subclavian arteries show significant stenosis of the vertebral arteries at their origin *(arrows)*. *C,* Corresponding subvolume MIP acquisition from 3D contrast-enhanced MR angiogram shows bilateral stenosis *(arrows)*, in accordance with findings at conventional angiography.

parameters of the sequence to obtain a fast 3D sequence with the highest spatial resolution and largest 3D volume possible without exceeding an acquisition time of 1 minute. The flip angle we chose was as long as possible to obtain better saturation of the surrounding structures, and we added a fat-saturation sequence to improve vascular contrast of the proximal great vessels. A zero-filling interpolation was used to improve spatial resolution. Flow compensation was not added in order to avoid a longer scan time. Despite a 6-cm slab thickness, the carotid siphons and the proximal portion of the great vessels were not assessable in about one third of our cases, owing to the limited coverage.

Good arterial enhancement was obtained in 80% of the patients and mild enhancement was achieved in the rest, but a second injection was required in 22% of the MR examinations. The contrast-infusion technique has been well documented in previous fast 3D MR angiographic studies of the abdominal aorta (12, 14–19). However, in head and neck imaging, the rapid venous enhancement, in which the blood-brain barrier may prevent extraction of gadolinium chelate from the intracerebral circulation, is a limiting factor of the technique. In the study by Levy et al (13), preferential enhancement of the cervical arteries was possible in 80% of their patients by using a single-dose bolus infusion and by choosing a delay such that the arterial phase occurred during acquisition of the central portion of k-space (24). In the present study, in which a 44-second acquisition time was used, the center of k-space was acquired in 22 seconds and, therefore, contrast agent was injected at the beginning of the sequence in most patients. Our longer scan time resulted in jugular vein enhancement in 81% of the patients, but this did not prevent image analysis. In patients requiring a second injection of contrast material, no adverse event was observed, which is consistent with a recent report evaluating the nephrotoxicity of high-dose contrast infusion (25). Methods have been described to optimize the timing of contrast material infusion. A test bolus of contrast can be administered before the acquisition (16) but this requires extra time and leads to residual venous enhancement. The 3D MR angiographic acquisition can be automatically triggered by a pulse sequence that detects the arrival of contrast material (14, 15) or fluoroscopically triggered in conjunction with an elliptical centric acquisition of k-space views (18). These more recent methods seem to be effective but are not available on most magnets. Moreover, a bolus timing error is mainly problematic for the assessment of the aorta and its branches owing to the shorter scan time related to the breath-holding technique.

The frequent overestimation of arterial narrowing and the three cases of signal void observed at the site of high-grade stenosis in our study may be explained by two main factors: first, the large voxel size allows intravoxel spin dephasing despite the short TE and contrast enhancement, and, second, severe stenosis may not be seen after MIP projection owing to the fact that the diameter of the residual lumen is close to the size of the voxel. A direct comparison of MIP reconstructions with source images could have improved the evaluation of carotid stenoses (26), but this was not possible because the data were acquired in the coronal plane, preventing an accurate analysis of the source images. An additional technique of reconstruction, such as multiplanar reformations,

TABLE 2: Proximal great vessels and carotid siphon: comparison between MR angiography and conventional angiography

	No. of Agreements/No. of Arteries			
	BCA (n = 15)	SCA (n = 40)	CCA (n = 33)	CS (n = 35)
Normal	14/14	37/37	30*/31	30/30
Mild stenosis	1/1	1†/2	1/1	0
Moderate stenosis	0	1/1	0	0
Severe stenosis	0	0	1/1	0
Occlusion	0	0	0	5/5
Total	15/15	39/40	32/33	35/35

Note.—BCA indicates brachiocephalic artery; SCA, subclavian artery; CCA, common carotid artery; CS, carotid siphon.

* One normal CCA on conventional angiograms was judged mildly stenotic on MR angiograms.

† One mildly SCA stenosis on conventional angiograms was judged moderately stenotic on MR angiograms.

TABLE 3: Internal carotid artery: comparison between conventional angiography and MR angiography

MR Angiography	Conventional Angiography				
	No Stenosis	Mild Stenosis	Moderate Stenosis	Severe Stenosis	Occlusion
No stenosis	**19**	0	0	0	0
Mild stenosis	1	**7**	2	0	0
Moderate stenosis	0	2	**6**	0	0
Severe stenosis	0	0	1	**10**	0
Occlusion	0	0	0	0	**6**
Total	20	9	9	10	6

TABLE 4: Vertebral artery: comparison between conventional angiography and MR angiography

MR Angiography	Conventional Angiography				
	No Stenosis	Mild Stenosis	Moderate Stenosis	Severe Stenosis	Occlusion
No stenosis	**39**	0	0	0	0
Mild stenosis	1	**4**	0	0	0
Moderate stenosis	2	0	**1**	0	0
Severe stenosis	0	0	1	**1**	0
Occlusion	0	0	0	0	**1**
Total	42	4	2	1	1

would be helpful to better define the degree of stenosis, but this requires extra postprocessing time.

The protocol used in the present study prevented the analysis of proximal great vessels and carotid siphons in 35% of the patients and led to a frequent overestimation of stenosis. However, despite these limiting factors, contrast-enhanced MR angiography was adequate for evaluating the territories in which atherosclerotic disease of the extracranial vessels occurs most frequently. Clinically relevant stenoses and occlusions of the ICA were correctly detected with very good sensitivity and specificity and good interobserver agreement. High-grade stenoses were clearly distinguished from occlusion despite a signal loss observed in the distal ICA in four cases of severe stenosis. This signal loss might be explained by the decreased flow leading to a reduced concentration of contrast agent in the distal arterial lumen. Only one moderate ICA stenosis seen at conventional angiography was judged as severe at MR angiography, and this might have led to a needless endarterectomy if MR angiography had been the sole technique used for imaging the cervical arteries. In the posterior circulation, evaluation of clinically relevant stenosis remains difficult with both duplex sonography and MR angiography, primarily because of the small diameter of the vertebral arteries and the frequent anatomic variations. Stenoses and occlusions were correctly detected, but three cases of normal vertebral arteries on conventional angiograms were misclassified as stenotic on MR angiograms, which may be attributed to the limited spatial resolution.

TABLE 5: Sensitivity and specificity of MR angiography for the evaluation of clinically relevant stenosis and ICA occlusion

	No. of Vessels	MR Angiography			
		Sensitivity (%)	Specificity (%)	PPV	NPV
ICA stenosis >70%	10	100	98	0.91	1.00
ICA occlusion	6	100	100	1.00	1.00
VA stenosis >50%	3	100	96	0.60	1.00

Note.—ICA indicates internal carotid artery; VA, vertebral artery; PPV, positive predictive value; NPV, negative predictive value.

Compared with the TOF technique, contrast-enhanced MR angiography may have some theoretical advantages: flow-related artifacts are minimized, any artery in the imaging volume can be visualized independently of its orientation, motion artifacts are rare because of the shorter scan time, and studies obtained in the coronal plane can depict both the carotid and vertebral arteries throughout their cervical and intracranial portions. However, conventional TOF MR angiography is probably superior for evaluating the percentage of stenosis of the carotid bifurcation owing to its inherent spatial resolution. An alternative protocol would be to use high-resolution 2D and 3D TOF imaging of the common carotid artery through the carotid siphon followed by an aortic arch study using the bolus contrast technique.

Conclusion

Although contrast-enhanced MR angiography is a promising technique that allows accurate evaluation of both carotid and vertebral arteries in most cases, the present protocol cannot be used as a stand-alone procedure for the evaluation of cervical atherosclerotic disease because of its low spatial resolution and inadequate anteroposterior coverage. These limiting factors will undoubtedly be overcome in the near

future. We are currently evaluating a new sequence with a reduced voxel size that is likely to provide a more accurate analysis of the supraaortic vessels.

Acknowledgments

We gratefully thank J. M. Franconi and L. Nicole for their helpful discussions, E. D'haese and J. Saulier for photographic reproductions, C. Rose and S. Rotsaert for help in preparing the manuscript, and the technical staff of the MR department for their support.

References

1. North American Symptomatic Carotid Endarterectomy Trial Collaborators. **Beneficial effect of carotid endarterectomy in symptomatic patients with high grade carotid stenosis.** *N Engl J Med* 1991; 325:445–453
2. European Carotid Surgery Trialists' Collaborative Group MRC. **European carotid surgery trial: interim results for symptomatic patients with severe (70–99%) or with mild (0–29%) carotid stenosis.** *Lancet* 1991;337:1235–1243
3. Hessel SJ, Adams DF, Abrams HL. **Complications of angiography.** *Radiology* 1981;138:273–281
4. Heiserman JE, Drayer BP, Fram EK, et al. **Carotid artery stenosis: clinical efficacy of two-dimensional time-of-flight MR angiography.** *Radiology* 1992;182:761–768
5. Huston J II, Lewius BD, Wiebert DO, Meyer FB, Riederer SJ, Weaver AL. **Carotid artery: prospective blinded comparison of two-dimensional time-of-flight MR angiography with conventional angiography and duplex US.** *Radiology* 1993;186:339–344
6. Mittl RL, Broderick M, Carpentier JP, et al. **Blinded-reader comparison of magnetic resonance angiography and duplex ultrasonography for carotid artery bifurcation stenosis.** *Stroke* 1994;25: 4–10
7. Vanninen RL, Manninen HI, Partanen KPL, Vainio PA, Soimakallio S. **Carotid artery stenosis: clinical efficacy of MR phase contrast flow quantification as an adjunct to MR angiography.** *Radiology* 1995;194;459–467
8. Prince MR. **Gadolinium-enhanced MR aortography.** *Radiology* 1994;191:155–164
9. Prince MR, Narasimham DL, Jacoby WT, et al. **Three-dimensional gadolinium-enhanced MR angiography of the thoracic aorta.** *AJR Am J Roentgenol* 1996;166:1387–1397
10. Cloft HJ, Murphy KJ, Prince MR, Brunberg JA. **3D gadolinium-enhanced MR angiography of the carotid arteries.** *Magn Reson Imaging* 1996;14:593–600
11. Yano T, Kodama T, Suzuki Y, Watanabe K. **Gadolinium-enhanced 3D time-of-flight MR angiography.** *Acta Radiol* 1997;38:47–54
12. Prince MR, Narasimham DL, Stanley JC, et al. **Breath-hold gadolinium-enhanced MR angiography of the abdominal aorta and its major branches.** *Radiology* 1995;197:785–792
13. Levy RA, Prince MR. **Arterial-phase three-dimensional contrast-enhanced MR angiography of the carotid arteries.** *AJR Am J Roentgenol* 1996;167:211–215
14. Prince MR, Chenevert TL, Foo TKF, Londy FJ, Ward JS, Maki JH. **Contrast-enhanced abdominal MR angiography: optimization of imaging delay time by automating the detection of contrast material arrival in the aorta.** *Radiology* 1997;203:109–114
15. Foo TKF, Saranathan M, Prince MR, Chenevert TL. **Automated detection of bolus arrival and initiation of data acquisition in fast, three-dimensional gadolinium-enhanced MR angiography.** *Radiology* 1997;203:275–280
16. Kim JK, Farb RI, Wright GA. **Test bolus examination in the carotid artery at dynamic gadolinium-enhanced MR angiography.** *Radiology* 1998;206:283–289
17. Kopka L, Vosshenrich R, Rodenwaldt J, Grabbe E. **Differences in injection rates on contrast-enhanced breath-hold three-dimensional MR angiography.** *AJR Am J Roentgenol* 1998;170:345–348
18. Wilman AH, Riederer SJ, King BF, Debbins JP, Rossman PJ, Ehman RL. **Fluoroscopically triggered contrast-enhanced three-dimensional MR angiography with elliptical centric view order: application to the renal arteries.** *Radiology* 1997;205:137–146
19. Siegelman ES, Gilfeather M, Holland GA, et al. **Breath-hold ultrafast three-dimensional gadolinium-enhanced MR angiography of the renovascular system.** *AJR Am J Roentgenol* 1997;168:1035–1040
20. Erickson SJ, Mewissen MW, Foley WD, et al. **Stenosis of the internal carotid artery, assessment using color Doppler imaging compared with angiography.** *AJR Am J Roentgenol* 1989;152:1299–1305
21. Fleiss JL. **Measuring nominal scale agreement among many raters.** *Psychol Bull* 1971;76:378–382
22. Siegel S, Castellan JJ. **Nonparametric Statistics for the Behavioral Sciences.** 2nd ed. New York: McGraw-Hill; 1988
23. Unger EC, Cohen MS, Gatenby RA, et al. **Single breath-holding scans of the abdomen using FISP and FLASH at 1.5 T.** *J Comput Assist Tomogr* 1988;12:575–583
24. Mezrich R. **A perspective on k-space.** *Radiology* 1995;195:297–315
25. Prince MR, Arnoldus C, Frisoli JK. **Nephrotoxicity of high-dose gadolinium compared with iodinated contrast.** *J Magn Reson Imaging* 1996;1:162–166
26. Anderson CM, Saloner D, Tsuruda JS, Shapeero LG, Lee RE. **Artifacts in maximum intensity projection display of MR angiograms.** *AJR Am J Roentgenol* 1990;154:623–629

Please see the Editorial on page 1184 in this issue.